

## Electronic Supporting Information

### **Interplay between structure and relaxation in polyurea networks: the point of view from a novel method of cooperativity analysis of dielectric response**

Nerea Sebastián,<sup>a,b</sup> Christophe Contal,<sup>c</sup> Antoni Sánchez-Ferrer,<sup>\*,d</sup> Marco Pieruccini<sup>\*,e</sup>

<sup>a</sup> *Jožef Stefan Institute, Department of Complex Matter - F7, Jamova cesta 39, SI-1000 Ljubljana, Slovenia.*

<sup>b</sup> *University of the Basque Country, Department of Applied Physics II, Apdo. 644, E-48080 Bilbao, Spain*

<sup>c</sup> *Institut Charles Sadron, Physics-Mechanics and Tribology of Polymers, 23 rue du Loess, BP 84047, F-67034 Strasbourg cedex, France.*

<sup>d</sup> *Swiss Federal Institute of Technology, Department of Health Sciences and Technology, IFNH, Schmelzbergstrasse 9, LFO, E29 CH-8092 Zürich, Switzerland.*

<sup>e</sup> *CNR, Istituto Nanoscienze, v. Campi 213/A, I-41125 Modena, Italy*

Corresponding author:

Marco Pieruccini ([marco.pieruccini@nano.cnr.it](mailto:marco.pieruccini@nano.cnr.it))

Antoni Sánchez-Ferrer ([antoni.sanchez@hest.ethz.ch](mailto:antoni.sanchez@hest.ethz.ch))

## Table of Contents

### Sample Characterization

**Figure S1:** Heat capacity measurements of the three polyurea elastomers around glass transition on heating.

**Figure S2:** SAXS (right) and WAXS (left) intensity profile for of the three elastomeric samples.

**Figure S3:** AFM height (left) and phase (right) profile image of the three bulk elastomeric samples.

**Figure S4:** AFM height (left) and phase (right) profile image of the three casted elastomeric samples.

**Figure S5:** 2D (left) and 1D FFT plot (right) of the two elastomeric samples.

### Broadband dielectric spectroscopy

**Figure S6:** Three-dimensional plot of the dielectric losses vs temperature and logarithm of the frequency for a) ED-2000 and b) ESD-2001.

**Figure S7:** Dielectric losses vs logarithm of the frequency for a) ED-2000 and b) ESD-2001 at different temperatures.

**Figure S8:** Fitting example for ED-2000.

**Figure S9:** Fitting example for ED-2001.

**Procedure for determination of the dc conductivity contribution from the electric modulus.**

**Figure S10:** Fitting example for ED-4000.

### Geometrical estimations

**Table S1:** Cooperativity values ( $N_\alpha$ ), radius of the cooperatively rearranging regions ( $R_{CRR}$ ), soft domain average distance ( $d_\alpha + d_{\alpha'}$ ), and thickness of the restricted

mobility layer ( $d_{\alpha'}$ ) at the temperature just above the glass transition temperature for the samples ED-2000 and ED-4000.

**Table S2:** Cooperativity values ( $N_{\alpha}$ ), radius of the cooperatively rearranging regions ( $R_{\text{CRR}}$ ), soft domain average distance ( $d_{\alpha} + d_{\alpha'}$ ), and thickness of the restricted mobility layer ( $d_{\alpha'}$ ) at -50 °C for the samples ED-2000 and ED-4000.

## Sample Characterization

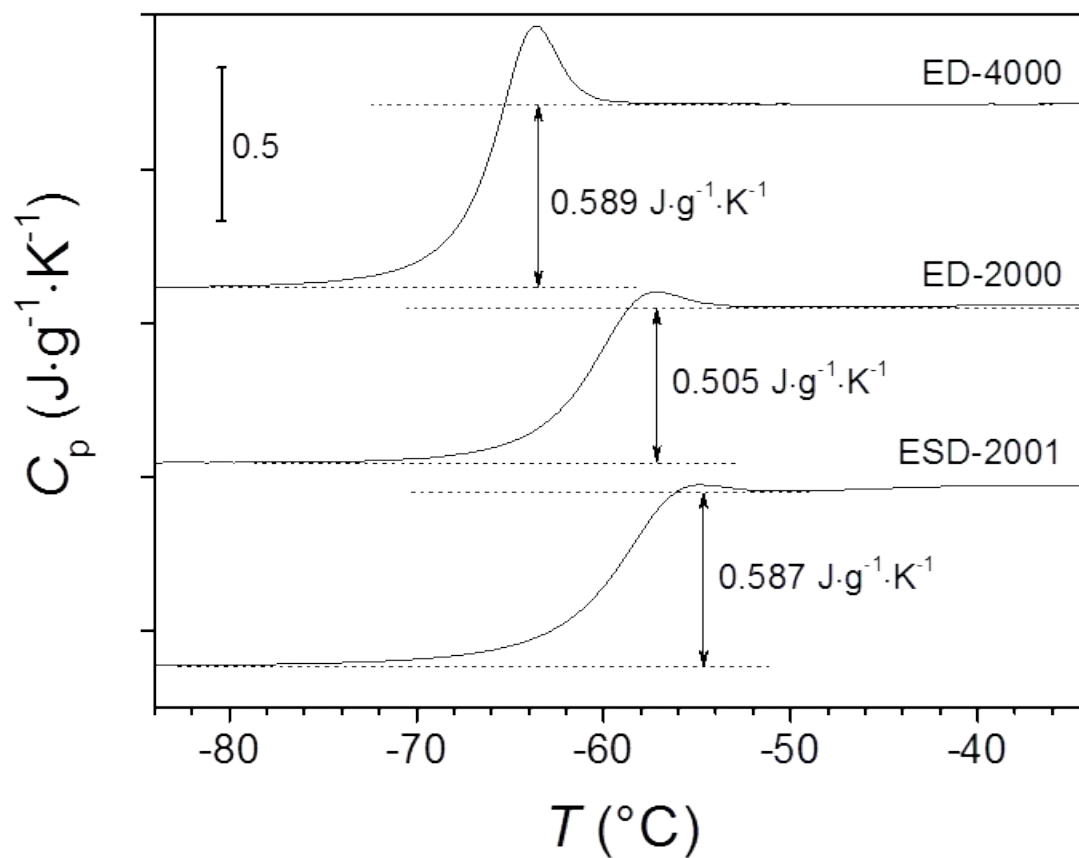


Figure S1. Heat capacity measurements of the three polyurea elastomers around glass transition on heating.

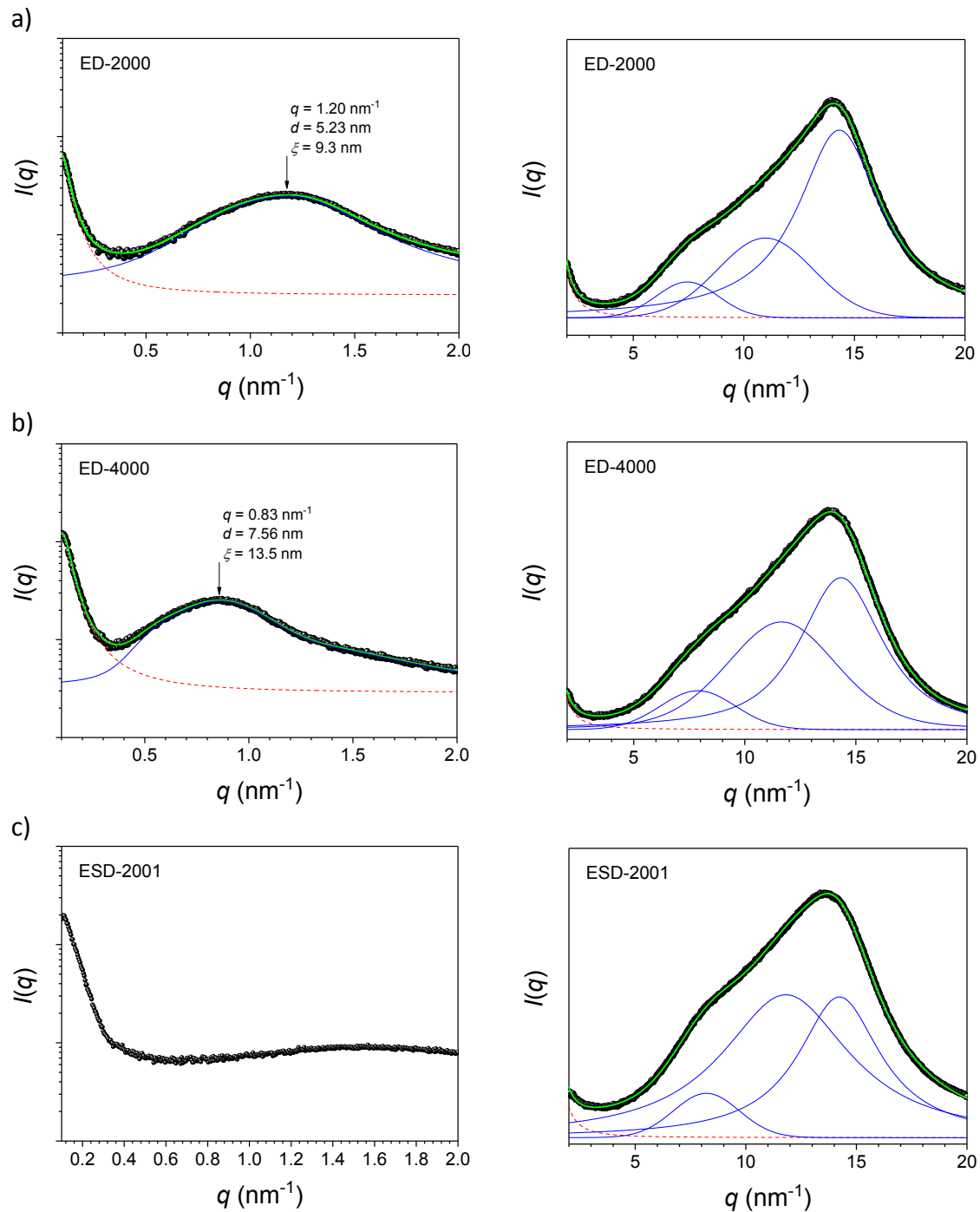


Figure S2: SAXS (left) and WAXS (right) intensity profile for of the three elastomeric samples a) ED-2000, b) ED-4000, and c) ESD-2001.

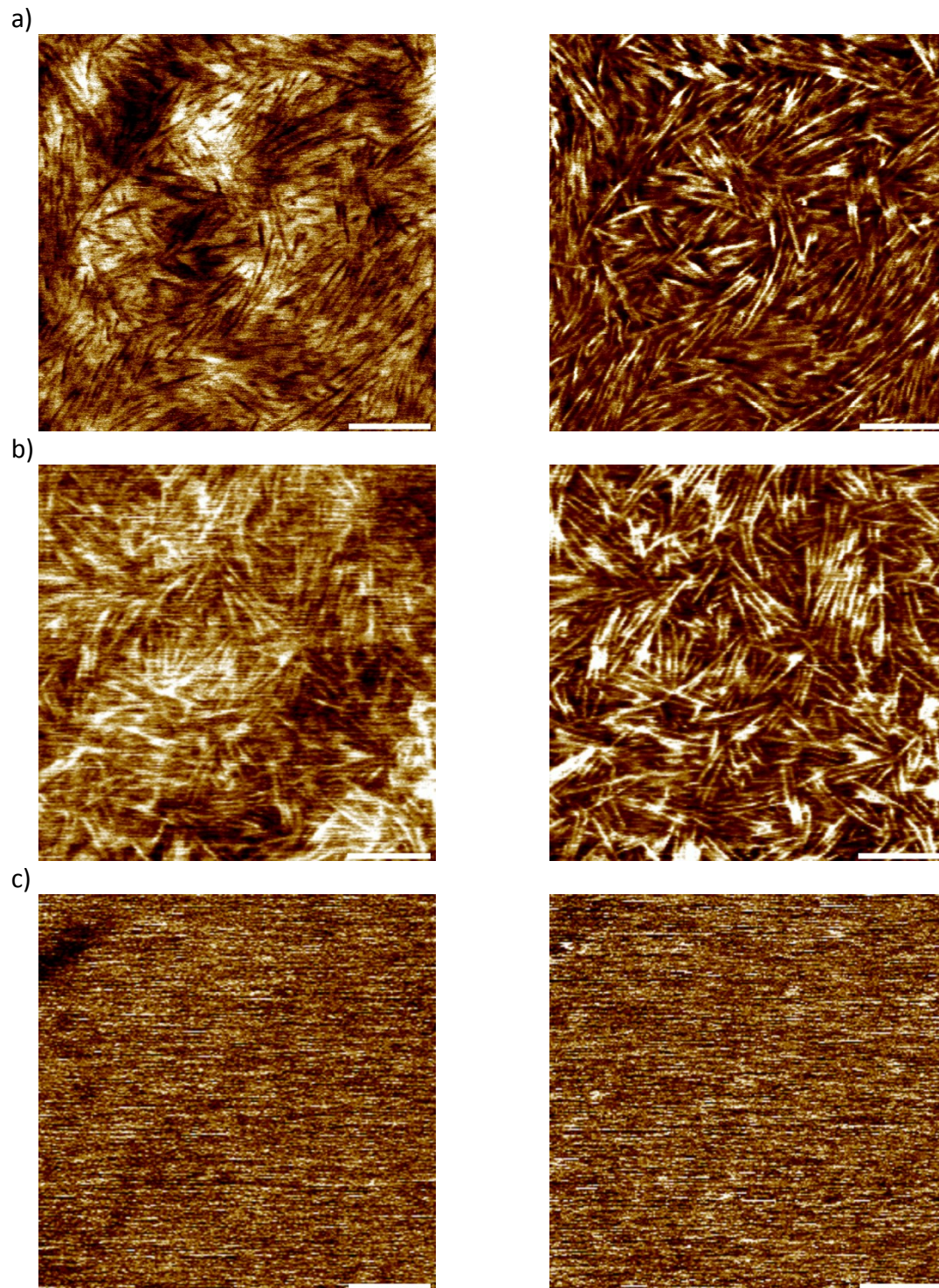


Figure S3. AFM height (left) and phase (right) profile image of the three bulk elastomeric samples a) ED-2000, b) ED-4000, and c) ESD-2001. *Note:* scale bar is 100 nm.

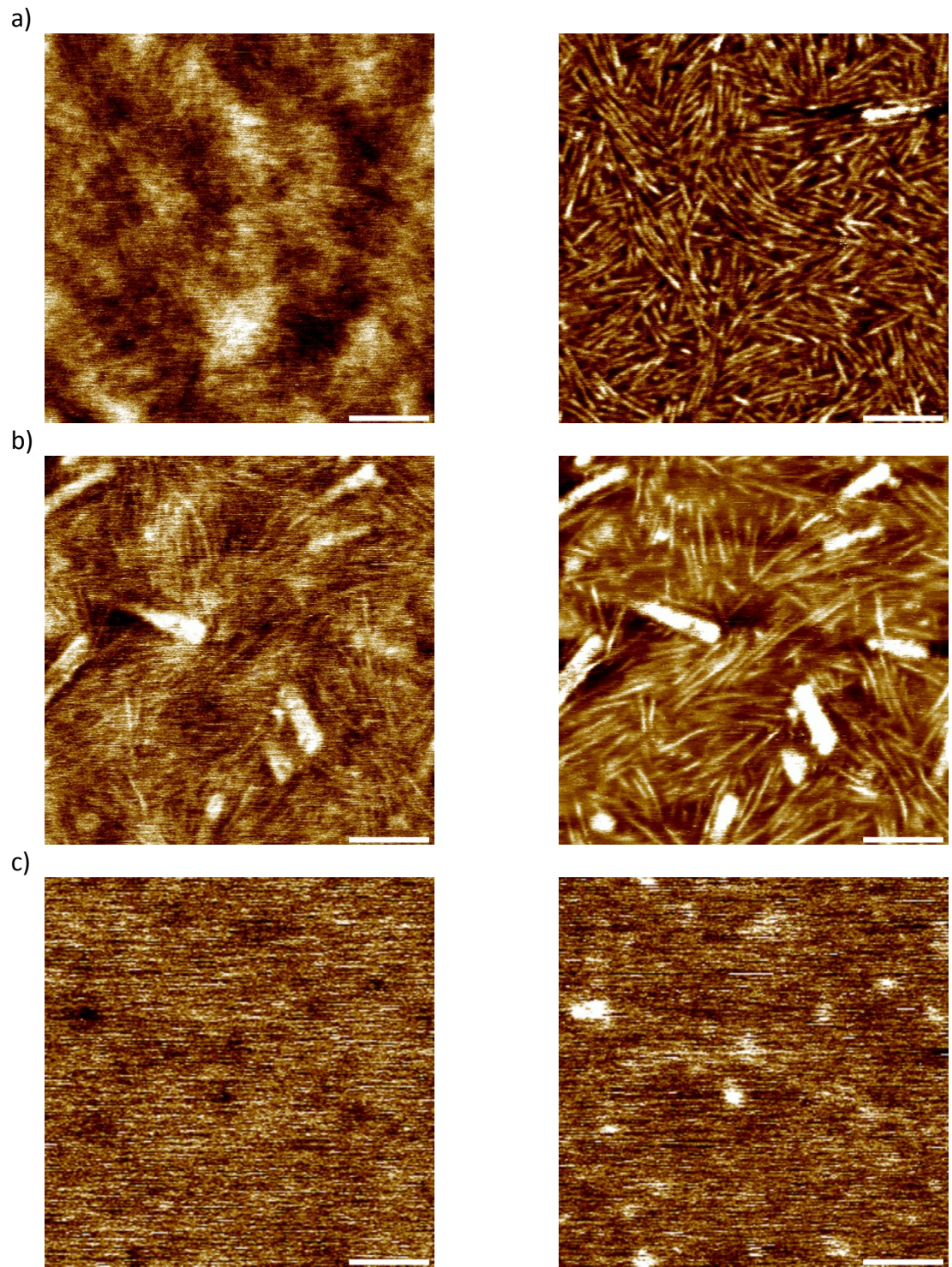


Figure S4. AFM height (left) and phase (right) profile image of the three casted elastomeric samples a) ED-2000, b) ED-4000, and c) ESD-2001. *Note:* scale bar is 100 nm.

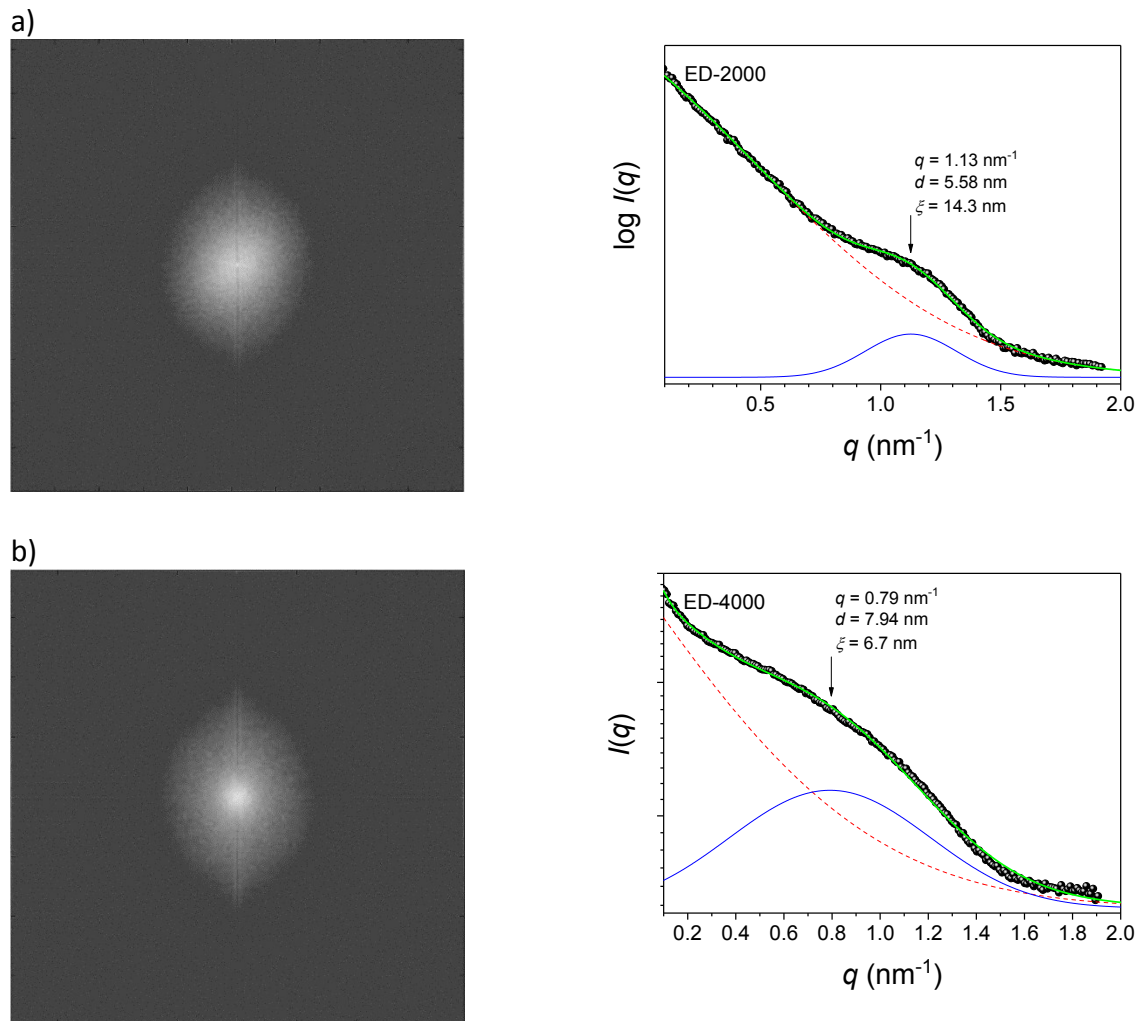
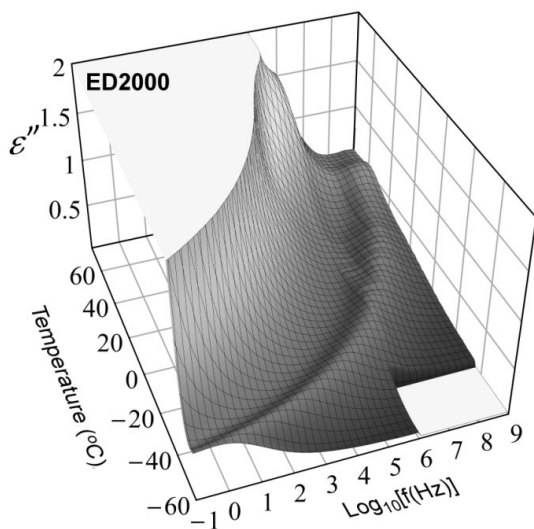


Figure S5. 2D (left) and 1D FFT plot (right) of the two elastomeric samples a) ED-2000, and b) ED-4000.



## Broadband dielectric spectroscopy

a)



b)

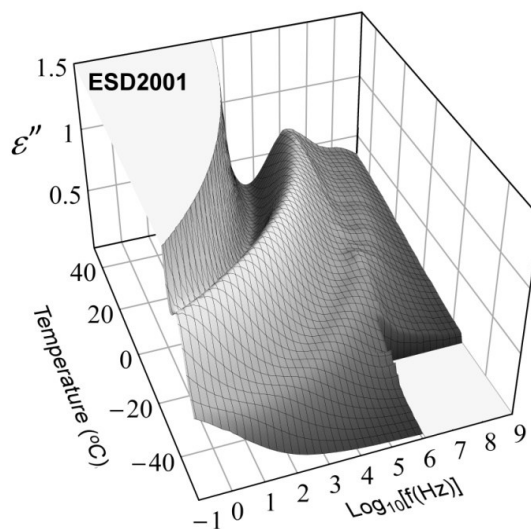
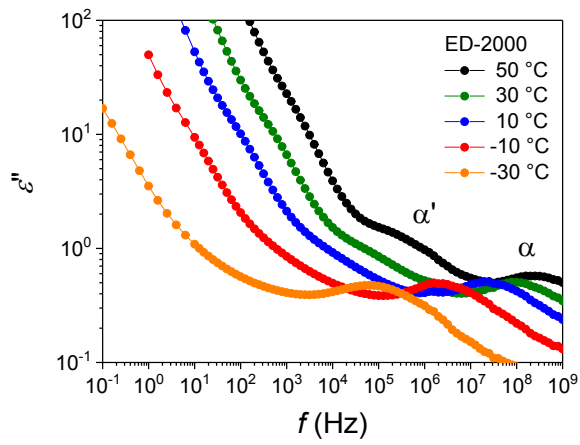


Figure S6. Three-dimensional plot of the dielectric losses vs temperature and logarithm of the frequency for a) ED-2000 and b) ESD-2001.

a)



b)

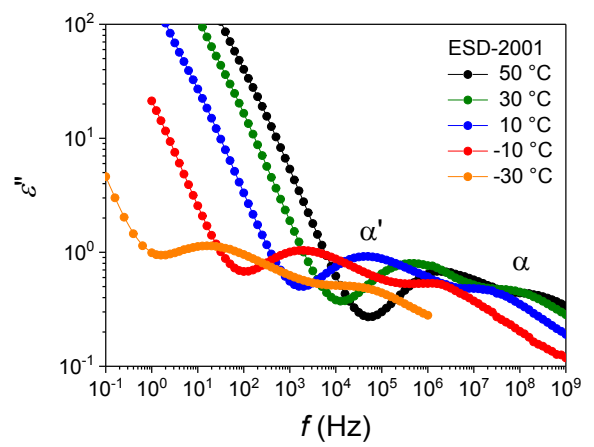


Figure S7. Dielectric losses vs logarithm of the frequency for a) ED-2000 and b) ESD-2001 at different temperatures.

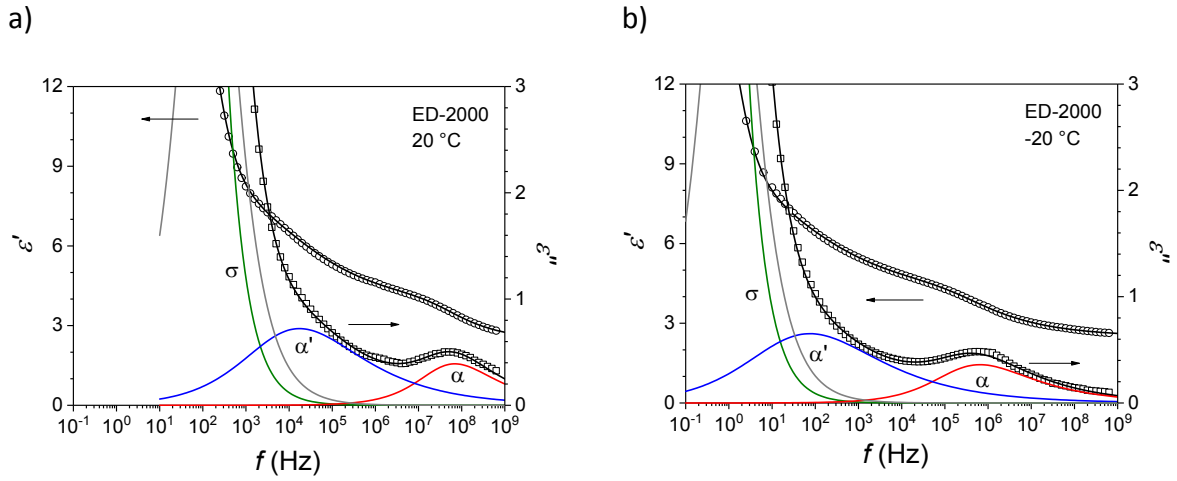
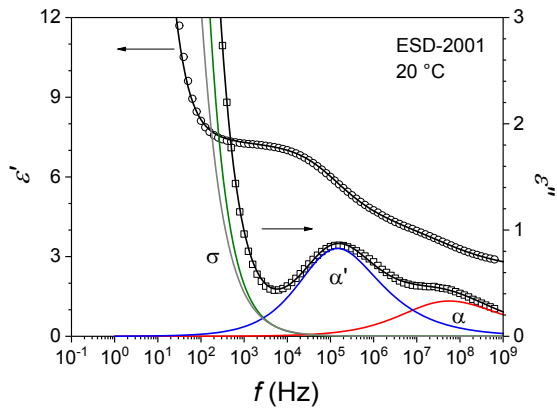


Figure S8. Real part (empty dots) and imaginary part (empty squares) of the dielectric permittivity versus frequency for ED-2000 at a) 20 °C and b) -20 °C. Solid black lines represent best fit to equation 1 (main text), and the color lines the deconvolution into the elementary modes  $\alpha$  and  $\alpha'$ . Green lines correspond to the dc conductivity contribution. Low frequency mode corresponds to MWS polarization.

a)



b)

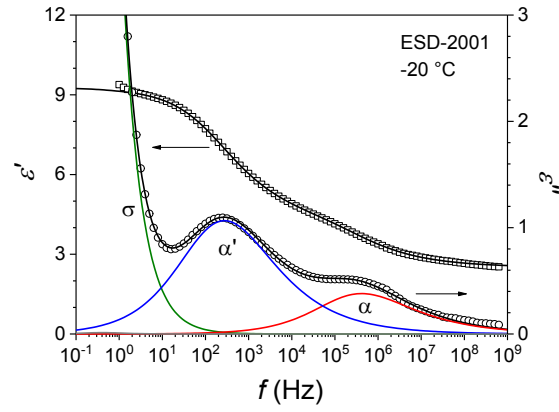


Figure S9. Real part (empty dots) and imaginary part (empty squares) of the dielectric permittivity versus frequency for ESD-2001 at a) 20 °C and b) -20 °C. Solid black lines represent best fit to equation 1 (main text), and the color lines the deconvolution into the elementary modes  $\alpha$  and  $\alpha'$ . Green lines correspond to the dc conductivity contribution. Low frequency mode corresponds to MWS polarization.

### Procedure for determination of the dc conductivity contribution from the electric modulus.

The complex electric modulus is defined as the inverse of the complex dielectric permittivity:

$$M^*(\omega) = 1 / \varepsilon^*(\omega) = M'(\omega) + iM''(\omega) \quad (\text{E1})$$

which gives

$$M'(\omega) = \frac{\varepsilon'(\omega)}{\varepsilon'^2(\omega) + \varepsilon''^2(\omega)} \quad (\text{E2})$$
$$M''(\omega) = \frac{\varepsilon''(\omega)}{\varepsilon'^2(\omega) + \varepsilon''^2(\omega)}$$

For pure dc-conductivity, there is no electronic conduction contribution to  $\varepsilon'(\omega)$ , while  $\varepsilon''(\omega) = \sigma_0 / \omega\varepsilon_0$ . It can be demonstrated that

$$M''(\omega) = M_\infty \frac{\omega\tau_{cond}}{1 + (\omega\tau_{cond})^2} \quad (\text{E3})$$

where  $\tau_{cond} = \varepsilon_0\varepsilon_\infty / \sigma_0$ . Equation E3 is comparable to the imaginary component of a Debye relaxation process.

The electric modulus can be fitted then to

$$M^*(\omega) = M_\infty + \frac{\Delta M_{cond}}{1 + (i\omega\tau_{cond})} + \sum_k \frac{\Delta M_k}{\left(1 + (i\omega\tau_{M,k})^{a_{M,k}}\right)^{b_{M,k}}} \quad (\text{E4})$$

where  $\tau_{M,k}$  are the characteristic relaxation times in the modulus representation and  $\Delta M_k$  are the amplitudes for the electric modulus given by the difference between the limiting low and high frequency values of each process. Parameters  $a_{M,k}$  and  $b_{M,k}$  stand for the symmetric and asymmetric broadening of the relaxation. It should be pointed out, that the shape parameters in E4 do not correspond to those of the permittivity representation in eq. 1 of the main text. By fitting the electric modulus to expression E4,  $\sigma_0$  can be determined as  $\varepsilon_0\varepsilon_\infty / \tau_{cond}$ . This value can then be fixed when performing the independent analysis of the complex dielectric permittivity according to equation 1 in main text. Examples of this approach are given in Figure S10.

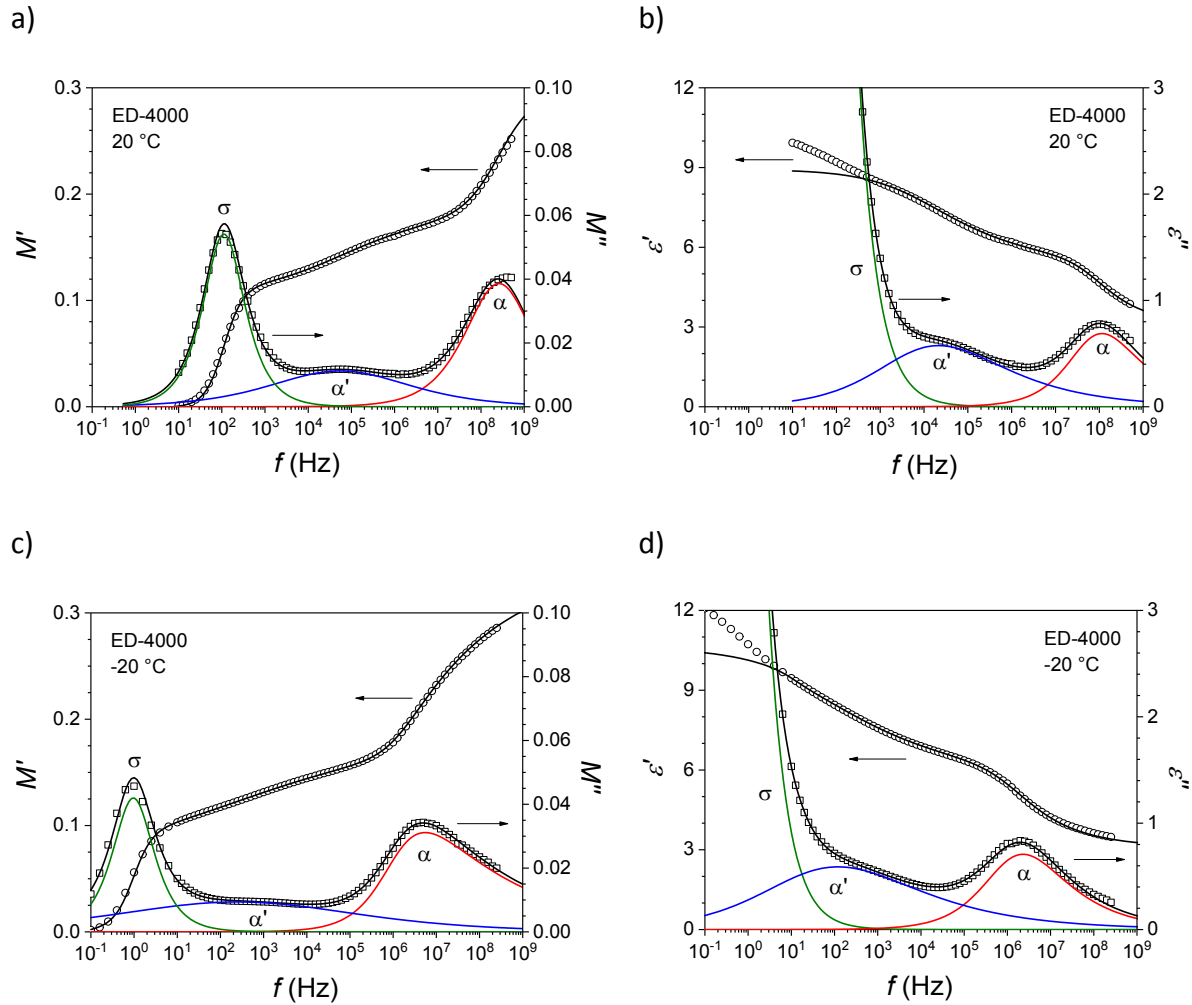


Figure S10. Real part (empty dots) and imaginary part (empty squares) of the electric modulus (a and c) and of the dielectric permittivity (b and d) versus frequency for ED-4000 at a) and b) 20 °C and c) and d) -20 °C. In the Modulus plots solid black lines represent best fit to Equation E4 (main text) and while in the permittivity plot they correspond to the results of independently fitting to equation 1 in the main text. Red and blue lines correspond to the deconvolution into the elementary modes  $\alpha$  and  $\alpha'$  obtained at each independent fit. Green lines correspond to the dc conductivity contribution.

Table S1. Cooperativity values ( $N_\alpha$ ), radius of the cooperatively rearranging regions ( $R_{\text{CRR}}$ ), soft domain average distance ( $d_\alpha + d_{\alpha'}$ ), and thickness of the restricted mobility layer ( $d_{\alpha'}$ ) at the temperature just above the glass transition temperature for the samples ED-2000 and ED-4000.

Sample	$N_\alpha$	$T$ (°C)	$R_{\text{CRR}}$ (nm)	SAXS		AFM	
				$d_\alpha + d_{\alpha'}$ (nm)	$d_{\alpha'}$ (nm)	$d_\alpha + d_{\alpha'}$ (nm)	$d_{\alpha'}$ (nm)
ED-2000	84	-60	1.25	3.32	0.41	3.54	0.52
ED-4000	80	-67	1.23	5.52	1.53	5.82	1.68

Table S2. Cooperativity values ( $N_\alpha$ ), radius of the cooperatively rearranging regions ( $R_{\text{CRR}}$ ), soft domain average distance ( $d_\alpha + d_{\alpha'}$ ), and thickness of the restricted mobility layer ( $d_{\alpha'}$ ) at -50 °C for the samples ED-2000 and ED-4000.

Sample	$N_\alpha$	$T$ (°C)	$R_{\text{CRR}}$ (nm)	SAXS		AFM	
				$d_\alpha + d_{\alpha'}$ (nm)	$d_{\alpha'}$ (nm)	$d_\alpha + d_{\alpha'}$ (nm)	$d_{\alpha'}$ (nm)
ED-2000	71	-50	1.18	3.32	0.48	3.54	0.59
ED-4000	49	-50	1.05	5.52	1.71	5.82	1.86